In vitro and *In vivo* Antitumor Effects of the Dual Insulin-Like Growth Factor-I/Insulin Receptor Inhibitor, BMS-554417

Paul Haluska,[1] Joan M. Carboni,[4] David A. Loegering,[2] Francis Y. Lee,[4] Mark Wittman,[5] Mark G. Saulnier,[5] David B. Frennesson,[5] Kimberly R. Kalli,[3] Cheryl A. Conover,[3] Ricardo M. Attar,[4] Scott H. Kaufmann,[2] Marco Gottardis,[4] and Charles Erlichman[1]

Divisions of [1]Medical Oncology, [2]Developmental Oncology Research, and [3]Endocrinology and Metabolism, Mayo Clinic College of Medicine, Rochester, Minnesota; [4]Oncology Drug Discovery, Pharmaceutical Research Institute, Bristol-Myers Squibb Co., Princeton, New Jersey; and [5]Discovery Chemistry, Bristol-Myers Squibb Co., Wallingford, Connecticut

Abstract

The insulin-like growth factor receptor (IGF-IR) and insulin receptor are either overactivated and/or overexpressed in a wide range of tumor types and contribute to tumorigenicity, proliferation, metastasis, and drug resistance. Here, we show that BMS-554417, a novel small molecule developed as an inhibitor of IGF-IR, inhibits IGF-IR and insulin receptor kinase activity and proliferation *in vitro*, and reduces tumor xenograft size *in vivo*. In a series of carcinoma cell lines, the IC_{50} for proliferation ranged from 120 nmol/L (Colo205) to >8.5 μmol/L (OV202). The addition of stimulatory ligands was unnecessary for the antiproliferative effect in MCF-7 and OV202 cells. BMS-554417 treatment inhibited IGF-IR and insulin receptor signaling through extracellular signal-related kinase as well as the phosphoinositide 3-kinase/Akt pathway, as evidenced by decreased Akt phosphorylation at Ser^{473}. At doses that inhibited proliferation, the compound also caused a G_0-G_1 arrest and prevented nuclear accumulation of cyclin D1 in response to LR3 IGF-I. In Jurkat T-cell leukemia cells, this agent triggered apoptotic cell death via the mitochondrial pathway. BMS-554417 was orally bioavailable and significantly inhibited the growth of IGF1R-Sal tumor xenografts *in vivo*. BMS-554417 is a member of a novel class of IGF-IR/insulin receptor inhibitors that have potential clinical applications because of their antiproliferative and proapoptotic activity *in vitro* and *in vivo*. (Cancer Res 2006; 66(1): 362-71)

Introduction

The insulin-like growth factor (IGF) system contains two receptor tyrosine kinases that are involved in propagating mitogenic signaling. The IGF receptor (IGF-IR) mediates proliferation when activated by the stimulatory ligands IGF-I and IGF-II (1–3). The insulin receptor is also a key component of the IGF signaling pathway. Although the classic insulin receptor isoform B only binds insulin and elicits metabolic effects, insulin receptor isoform A binds IGF-2 in addition to insulin and initiates mitogenic signaling (4). In normal cells, activation of IGF-IR and insulin receptor is tightly regulated by the action of IGF binding proteins (IGFBP) and the nonstimulatory receptor IGF-IIR. Dysregulation of the IGF-I system has been implicated in the proliferation of numerous neoplasms, including multiple myeloma, as well as breast, prostate, colon, ovarian, and lung cancers (5, 6). IGF-I signaling also seems to play a vital role in malignant transformation, metastasis, angiogenesis, and the development of resistance to clinically useful anticancer treatments, including hormonal agents, biological growth factor inhibitors, radiation, and cytotoxic chemotherapy (7–13).

According to current understanding, activation of IGF-IR and insulin receptor antagonizes apoptotic cell death. In particular, signaling by these receptors activates the serine/threonine kinase Akt, which phosphorylates a series of polypeptides that regulate both of the major caspase activation pathways (14). Akt-mediated inhibition of the mitochondrial pathway reflects phosphorylation and sequestration of the proapoptotic Bcl-2 family member Bad (15), altered synthesis of microtubule-associated BH3 only protein Bim (16), effects on other mitochondrial polypeptides that regulate cytochrome *c* release (17), and possible modification of procaspase-9 (18). Due to its critical role in IGF-I-mediated mitogenesis and inhibition of apoptosis, the IGF-IR has been a major focus for the development of novel anticancer therapies. Inhibition of the IGF-IR by a variety of strategies has shown activity in a wide range of hematologic and solid tumors *in vitro* and *in vivo* (19). Although the insulin receptor plays a critical stimulatory role in the IGF-I system, most strategies have been deliberately designed for selectivity against the IGF-IR and not the insulin receptor, due to potential metabolic consequences of inhibiting the latter. However, emerging data suggest that elevated levels of insulin receptor isoform A and IGF-II in certain cancers may establish an autocrine growth loop (6, 20–22). In addition to proliferative effects, the insulin receptor may influence migration, differentiation, and survival (4, 22–24). Furthermore, IGF-IR and insulin receptor isoform A can form hybrid receptors that bind IGF-I and IGF-II at physiologic concentrations, suggesting that inhibition of both receptors may necessary for inhibiting IGF-mediated proliferation (4, 20).

Here, we report the effects of BMS-554417, a member of a class of inhibitors identified as part of a drug discovery program aimed at developing small molecule inhibitors of the IGF-IR. BMS-554417 inhibits both the insulin receptor and IGF-IR with similar potency in both cell-free and intact cell assays. Further analysis indicates that BMS-554417 affects cell proliferation by inhibiting Akt and extracellular signal-related kinase (ERK) activation and prevents nuclear accumulation of cyclin D1 at the G_1-S transition as well as inducing apoptosis via the mitochondrial pathway. BMS-554417 administered orally also has significant activity *in vivo* and leads to temporary hyperglycemia at efficacious doses (25).

Materials and Methods

Reagents were obtained from the following suppliers: bovine serum albumin (BSA), β-estradiol, Hoechst 33258, human recombinant insulin, and

Requests for reprints: Charles Erlichman, Division of Medical Oncology, Guggenheim 1311, Mayo Clinic, 200 First Street Southwest, Rochester, MN 55905. Phone: 507-284-3514; Fax: 507-266-5146; E-mail: erlichman.charles@mayo.edu.

doi:10.1158/0008-5472.CAN-05-1107

Protein A-Sepharose CL-4B from Sigma (St. Louis, MO); SDS-PAGE reagents from Bio-Rad (Hercules, CA); fetal bovine serum (FBS) and trypsin-EDTA from Life Technologies/Invitrogen (Grand Island, NY); LongR^3 IGF-I (LR3 IGF-I) from Gro Pep (Thebarton, South Australia, Australia); IETD(OMe)-fmk from ICN (Irvine, CA); zVAD(OMe)-fmk from Biomol (Plymouth Meeting, PA); Protease Inhibitor Cocktail Set III from Calbiochem (San Diego, CA); and CellTiter 96 Non-Radioactive Cell Proliferation Assay Kit from Promega (Madison, WI). Polyclonal antibodies were obtained from the following suppliers: insulin receptor β-subunit (C-I9), IGF-IR β-subunit, and actin from Santa Cruz Biotechnology (Santa Cruz, CA); Akt, phospho-Akt pSer^{473}, ERK1/2, phospho-ERK1/2 pThr^{202}/pTyr^{204}, phospho-IGF-IR pTyr^{1131}/insulin receptor pTyr^{1146}, stress-activated protein kinase/c-Jun NH_2-terminal kinase (SAPK/JNK), p38, and phospho-p38 pThr^{180}/pTyr^{182} from Cell Signaling Technology (Beverly, MA); phospho-Akt1 pThr^{308}, cyclin D1, phospho-FAK pTyr^{397} from Upstate Biotechnology (Lake Placid, NY); and anti-Bcl-x_L from DAKO (Carpinteria, CA).

Monoclonal antibodies were obtained from the following suppliers: phospho-SAPK/JNK pThr^{183}/pTyr^{185} and phospho-tyrosine (p-Tyr^{100}) from Cell Signaling Technology; IGF-IRβ and focal adhesion kinase (FAK) from Upstate Biotechnology; and insulin receptor β-subunit (29B4) from Santa Cruz Biotechnology. Monoclonal antibody to poly(ADP-ribose) polymerase-1 (PARP-1) was a kind gift from Guy Poirier (Laval University, Ste-Foy, Quebec). Peroxidase-coupled secondary antibodies were supplied by Pierce (Rockford, IL). Fluorescein-labeled affinity purified antibody to rabbit IgG was supplied by KPL (Gaithersburg, MD).

Kinase assays. To assess the specificity of BMS-554417, the activities of various baculovirus-expressed kinases were assayed by measuring the incorporation of radiolabeled ATP into synthetic peptides or protein substrates. The reactions were done in 96-well plates and included relevant kinase, substrate, ATP, and appropriate cofactors at concentrations optimized for each individual kinase. Reactions were stopped by the addition of trichloroacetic acid. After the precipitates were collected onto GF/C unifilter plates (Packard Instrument Co., Meriden, CT) using a Filtermate universal harvester (Packard Instrument), the filters were quantitated using a TopCount 96-well liquid scintillation counter (Packard Instrument). The ability of BMS-554417 to inhibit each kinase was determined by comparing counts incorporated in the presence of various concentrations of compound with those incorporated in the absence of compound. The concentration of BMS-554417 that achieved IC_{50} of each kinase activity was calculated from nonlinear regression analysis using GraphPad Prism version 3.00 for Windows (GraphPad Software, San Diego, CA).

Cell cultures. MCF-7 breast cancer cells from American Type Culture Collection (ATCC, Manassas, VA) were cultured in DMEM containing penicillin (100 units/mL), streptomycin (100 μg/mL), sodium pyruvate (1 mmol/L), and 10% FBS. The OV202 epithelial ovarian cancer cell line was derived from a primary tumor specimen as described previously (20) and propagated in MEM containing penicillin (100 units/mL), streptomycin (100 μg/mL), and 10% FBS. The above media constituted "complete" media. Serum-deficient or serum-free media were prepared as above but contained 1% and 0% FBS, respectively. Jurkat human T-cell leukemia cells were a gift from Paul Leibson (Mayo Clinic, Rochester, MN). I2.1 cells, which lack FADD (26), were purchased from ATCC. JB-6 cells, which lack caspase-8 and overexpress Bcl-2 (27), were kindly provided by Shigekazu Nagata (Kyoto University, Kyoto, Japan). To derive Bcl-x_L overexpressing clones, Jurkat cells were transfected with the plasmid spleen focus-forming virus (SSFV)/Bcl-x_L (a gift from Andrew Badley, Mayo Clinic), which contains the Bcl-xL cDNA behind the SSFV long terminal repeat, using a BTX 820 square wave electroporator operating at 240 V for 10 milliseconds. After a 48-hour incubation to allow transgene expression, cells were selected in 400 μg/mL G418 and cloned by limiting dilution. Expression of Bcl-x_L in various clones was assessed by immunoblotting. Jurkat cells and their variants in log-phase culture were diluted to 1.2×10^5/mL in RPMI 1640 containing 15% FCS, 100 units/mL penicillin G, 100 μg/mL streptomycin, and 2 mmol/L glutamine. Cell lines used in Fig. 2*C* were obtained from ATCC and cultured per supplied protocols.

3-(4,5-Dimethylthiazol-2-yl)-5-(3-carboxymethoxyphenyl)-2-(4-sulfophenyl)-2*H*-tetrazolium assay. 3-(4,5-Dimethylthiazol-2-yl)-5-(3-carboxymethoxyphenyl)-2-(4-sulfophenyl)-2*H*-tetrazolium (MTS) assays were done as previously described with modifications (28). Cells grown to 70% to 80% confluence were trypsinized and seeded at 5,000 per well in a 96-well plate in complete medium overnight. The medium was then changed to serum-deficient medium containing either the growth factor diluent (10 mmol/L HCl/0.1% BSA), LR3 IGF-I (10 nmol/L), or insulin (10 nmol/L) and increasing concentrations of BMS-554417 for 72 hours at 37°C. Three or four replicate wells were exposed to each condition. Untreated cells served as controls. Plates were then assayed using the CellTiter 96 MTS/Proliferation Assay kit according to the product manual. Absorbance was read at 570 nm, and cell numbers were calculated against a standard curve. Experiments were repeated at least four times.

Thymidine incorporation assay. Cells were plated in 96-well plates and, 24 hours later, were exposed to a range of drug concentrations. After 72 hours at 37°C, cells were pulsed with 4 μCi/mL [6-^{3}H]thymidine (Amersham Pharmacia Biotech, Little Chalfont, United Kingdom) for 3 hours, trypsinized, harvested onto UniFilter-96, GF/B plates (Perkin-Elmer, Boston, MA), and counted on a TopCount.NXT (Packard Instrument) scintillation counter. Results are expressed as an IC_{50}, which is the drug concentration required to inhibit cell proliferation by 50% compared with that of untreated control cells.

Western blotting and immunoprecipitation. Cells grown to 70% to 80% confluence were switched to serum-free medium for 24 hours. Replicate plates were then exposed to serum-free medium, DMSO, or BMS-554417 for 1 hour at the approximated IC_{80} concentration (MCF-7, 5 μmol/L; OV202, 20 μmol/L). Fifteen minutes before the end of the 1-hour exposure, either ligand diluent (10 mmol/L HCl/0.1% BSA), LR3 IGF-I (10 nmol/L), or insulin (10 nmol/L) was added to the cells. Cells were washed twice with ice-cold PBS, then lysed in 4× sample buffer [250 mmol/L Tris-HCl (pH 6.8), 8% SDS, 20% glycerol, 0.0075% bromphenol blue] or radioimmunoprecipitation assay (RIPA) buffer [50 mmol/L Tris-HCl (pH 7.4), 150 mmol/L NaCl, 0.5% NP40, 0.5% Triton X-100, 0.25% sodium deoxycholate with freshly added 10 mmol/L sodium pyrophosphate, 1 mmol/L NaF, 1 mmol/L sodium orthovanadate, 2 mmol/L phenylmethylsulfonyl fluoride, 1 mmol/L AEBSF, 800 nmol/L aprotinin, 50 μmol/L bestatin, 15 μmol/L E-64, 20 μmol/L leupeptin, and 10 μmol/L pepstatin A]. Lysates were then sonicated and frozen immediately at −20°C or assayed for total protein by the bicinchoninic acid method (29) and immediately used for immunoprecipitation. For Western blotting, samples were boiled at 95°C for 15 minutes with 100 mmol/L DTT and separated by SDS-PAGE. After proteins were transferred to nitrocellulose or polyvinylidene difluoride, membranes were blocked for 1 hour in PBS-T/5% nonfat milk or BSA and probed overnight at 4°C with primary antibodies. After three washes in PBS-T, blots were probed with horseradish peroxidase–conjugated secondary antibody for 1 hour. After three additional washes, bands were visualized with enhanced chemiluminescence reagent (Amersham, Piscataway, NJ) on XoMAT film (Kodak, Rochester, NY).

For immunoprecipitations, 1,000 to 2,000 μg of protein diluted to 1 mL with RIPA buffer was centrifuged at 10,000 × *g* for 10 minutes at 4°C to remove cellular debris. The supernatant was precleared with 20 μL of a 50% slurry of Protein A-Sepharose and 1.0 μg of control anti-rabbit or anti-mouse IgG for 30 minutes at 4°C. After samples were centrifuged at 1,000 × *g* for 30 seconds at 4°C, the supernatant was removed and treated with 4 μg of anti-IGF-IRβ (Upstate Biotechnology) or 2 μg anti-IRβ (29B4; Santa Cruz Biotechnology) with 20 μL of a 50% Protein A-Sepharose slurry for 2 hours at 4°C. The immunoprecipitates were collected by centrifugation at 1,000 × *g* for 30 seconds, washed twice with RIPA buffer, solubilized by boiling for 15 minutes in 4× sample buffer/100 mmol/L DTT, loaded onto SDS-PAGE gels, and processed for Western blotting as above. Experiments were repeated at least thrice.

Cell cycle/fluorescence-activated cell sorting analysis. MCF-7 cells were grown to ~70% confluence in complete medium, washed, and incubated for 72 hours in serum-free/phenol red-free medium ("free" medium). Cells were then incubated for an additional 24 hours in serum-free medium with diluent or LR3 IGF-I (10 nmol/L) ± BMS-554417 at IC_{90}

(5 μmol/L). After 24 hours, cells were trypsinized, washed in ice-cold PBS, pelleted by centrifugation at 600 × *g* for 10 minutes, resuspended in PBS, and fixed for at least 12 hours with an equal volume of 95% ethanol. Cells were rehydrated with ice-cold PBS, treated with 1 mg/mL RNase A in 0.1% sodium citrate for 15 minutes at 37°C, stained with 50 μg/mL propidium iodide for 15 minutes at room temperature in the dark, and immediately analyzed using a FACScan cytometer (Becton Dickinson, San Jose, CA); 20,000 events were collected and analyzed using ModFit LT software (Verify Software, Topsham, ME). Experiments were repeated at least thrice.

Immunocytohistochemistry. MCF-7 cells seeded onto sterile slides or slide chambers and were grown and treated as in the previous section. After fixation and permeabilization in acetone for 15 minutes at 20°C, slides were washed four times with PBS and blocked in TSM [150 mmol/L NaCl, 10 mmol/L Tris-HCl (pH 7.4), 10% nonfat milk, 100 units/mL penicillin, 100 μg/mL streptomycin, 1 mmol/L sodium azide]. Slides were incubated in anti-cyclin D1 at 20 μg/mL in TSM for 48 hours at 4°C, washed with PBS, incubated with fluorescein-conjugated anti-rabbit IgG in TSM for 1 hour at 4°C, washed again with PBS, incubated with Hoechst dye 33258 (1 μg/mL) for 15 minutes at room temperature, mounted, and examined using a Zeiss LSM 510 Confocal Laser Scanning Microscope.

Apoptosis induction. Solid tumor cell lines were grown to 70% confluence in complete medium. After 24 hours of incubation in serum-deficient medium, cells were treated with BMS-554417 at the IC_{90} concentration or diluent in serum-deficient medium for an additional 72 hours. Serum-deficient medium was used in lieu of serum-free medium to avoid serum deprivation–induced apoptosis. At the end of the treatment, adherent cells were released by trypsinization, combined with nonadherent cells, and recovered by centrifugation at 600 × *g* for 5 minutes at 4°C. Samples for SDS-PAGE were washed twice with ice-cold PBS, lysed in 200 μL of 4× sample buffer/100 mmol/L DTT, and boiled for 15 minutes at 95°C. Samples for morphologic examination were fixed for >12 hours in 3:1 methanol/acetic acid, applied to glass coverslips, stained with 1 μg/mL Hoechst 33258 in 50 mmol/L Tris-HCl (pH 7.4 at 21°C) containing 50% (v/v) glycerol, and examined by fluorescence microscopy for apoptotic morphologic changes, such as chromatin condensation and nuclear fragmentation (30). After addition of potential modulating agents as indicated in the figure legends, Jurkat cells were treated for 72 hours with the indicated BMS-554417 concentration or, as a control, 0.1% DMSO before examination for apoptotic morphologic changes as indicated above. Approximately 500 cells per slide were counted.

Murine tumor allograft models. IGF1R-Sal tumors were generated as previously described (31). Briefly, ~20 mg of established tumor was injected s.c. into eight nude mice per treatment group using a 13-gauge trocar and allowed to propagate to a target volume of 1,000 mm^3 as determined by caliper measurements. Treatment was initiated in each mouse once tumors reached a volume of ~100 mm^3, which was calculated using the formula $(L \times W^2) / 2$. Animals were then treated with either vehicle alone (80% polyethylene glycol 400 in water) alone or with BMS-554417. All animal procedures were approved by the Bristol-Myers Squibb (BMS) Institutional Animal Care and Use Committee. The animal care and use program at BMS has been fully accredited by the Association for Assessment and Accreditation of Laboratory Animal Care International (Rockville, MD).

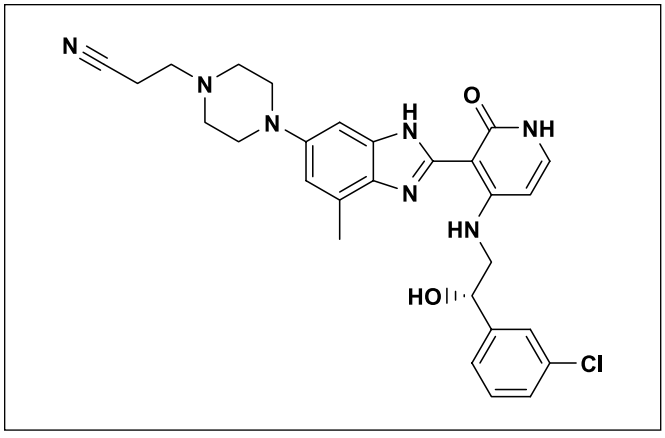

Figure 1. Chemical structure of BMS-554417.

Table 1. *In vitro* inhibitory activity and selectivity of BMS-554417

Enzyme	IC_{50}, nmol/L (95% confidence interval)
IR	50.6 (44.6-57.4)
IGF-1R	67.9 (53.1-86.9)
FAK	94.0 (85.7-103)
MEK	356 (217-583)
Emt	346 (288-416)
PKCα	397 (340-463)
Syk	615 (422-897)
VEGFR2	>1,000
Lck	>1,500
PKCδ	>2700
Her1	>3,000
p38	>10,000
CDK2	>10,000
HER2	>10,000
PDE 3	>17,000
CaMKII	>20,000
Akt	>20,000
GSK 3	>27,000
PDE 4	~40,000
PDE 7	~40,000

NOTE: *In vitro* kinase assays were done with the purified recombinant kinases in the absence or presence of increasing concentrations of BMS-554417, as described in Materials and Methods.

IC_{50} represents the calculated mean value for the concentration of BMS-554417 that inhibits the ability of each kinase to phosphorylate its synthetic substrate by 50%. Ninety-five percent confidence intervals shown for IC_{50} <1,000 nmol/L.

Abbreviations: IR, insulin receptor; PKC, protein kinase C; CaMKII, calcium/calmodulin-dependent protein kinase II; MEK, mitogen-activated protein kinase kinase; PDE, phosphodiesterase; CDK2, cyclin-dependent kinase 2; GSK 3, glycogen synthase kinase 3.

Oral glucose tolerance test. After a 2-hour fasting period, nude mice were dosed orally with vehicle with or without BMS-554417 at a single dose 4 hours before an oral glucose challenge (1 g/kg). Serum glucose was monitored at 0, 15, 30, 60, 90, and 120 minutes after glucose challenge using a blood glucometer (Elite XL, Bayer, Elkhart, IN). Serum insulin was measured at 120 minutes post glucose challenge by ELISA (INSSKR020, Crystal Chem, Downers Grove, IL).

Serum BMS-554417 determinations. After removal of plasma protein by acetonitrile extraction, samples were separated by reverse-phase high-performance liquid chromatography using a dual mobile-phase system. Upon sample injection, the mobile-phase composition changed linearly from initial [85% A (10 mmol/L ammonium formate/0.1% formic acid in water)/15% B (10 mmol/L ammonium formate/0.1% formic acid in 10% water/90% acetonitrile)] to 15% A/85% B over 2 minutes, where it was then held for two additional minutes. The resolved compound was identified and quantified using a Micromass Quattro LC tandem mass spectrometer against a standard curve.

Statistical analysis. For statistical analysis, the Student's *t* test was used for pairwise comparisons. Gehan's generalized Wilcoxon test was

used for nonparametric comparison of *in vivo* tumor growth delay to target volume. The Kruskal-Wallis test was used for pairwise comparisons of *in vivo* tumor volume. Results were considered significant at $P < 0.05$.

Results

BMS-554417 shows selectivity towards IGF-IR and insulin receptor *in vitro*. BMS-554417 is a 2-(4-substituted-2-oxo-1,2-dihydropyridin-3-yl)-benzimidazole derivative that has selectivity towards the IGF-IR and insulin receptor (Fig. 1; Table 1; ref. 32). BMS-554417 inhibited IGF-IR kinase activity with an IC_{50} of 68 nmol/L. Similarly, it was also a potent inhibitor of insulin receptor and FAK kinase activity with IC_{50} values of 51 and 94 nmol/L, respectively. BMS-554417 displayed ≥5-fold selectivity over other kinases assayed, as shown in Table 1. The insulin receptor and IGF-IR kinases were the only receptor tyrosine kinases inhibited at submicromolar concentrations.

BMS-554417 inhibits proliferation in a dose-dependent manner and in multiple tissue types. To assess activity of BMS-554417 in tumor cell lines, the IC_{50} and IC_{90} concentrations were determined using MTS assays (Fig. 2). These assays were done in the absence or presence of insulin (10 nmol/L) or LR3 IGF-I (10 nmol/L), an IGF-I analogue that activates IGF-IR irrespective of IGFBP levels (33). MCF-7 cells exhibited a dose-dependent decrease in MTS dye reduction compared with untreated cells (Fig. 2*A*). The IC_{50} for this antiproliferative effect was in the submicromolar range with or without added ligands.

OV202 cells also exhibited a dose-dependent inhibition of proliferation but were 18- to 42-fold less sensitive to BMS-554417 compared with MCF-7 cells (Fig. 2*B*). There was no significant difference in the sensitivity of OV202 cells to BMS-554417 in the presence of either LR3 IGF-I or insulin versus no growth factor at any concentration tested.

In a panel of human tumor cell lines, the IC_{50} of BMS-554417 ranged from 146 nmol/L to 2.21 μmol/L (Fig. 2*C*). Although differential sensitivity was seen among the different tumor types, the colon cancer cell lines tested were relatively more sensitive as a group. The sarcoma and breast cancer cell lines tested had a greater than a log-fold range in sensitivity as measured by thymidine incorporation. The prostate cancer cell lines showed a nearly log-fold range of sensitivity.

BMS-554417 inhibits IGF-IR and insulin receptor phosphorylation in intact cells. To show the ability of BMS-554417 to inhibit the activity of the IGF-IR and insulin receptor tyrosine kinase in intact cells, receptor phosphorylation was examined in the presence or absence of drug and stimulatory ligands (Fig. 3). IGF-IR and insulin receptor were immunoprecipitated from treated cells and analyzed by Western blotting using a phosphotyrosine-specific antibody. In MCF-7 cells (Fig. 3*A*), there was no detectable phosphorylation of the immunoprecipitated IGF-IR and insulin receptor without the addition of growth factors. However, in the presence of growth factors LR3 IGF-I (10 nmol/L) or insulin (25 nmol/L), there was detectable phosphorylation of the IGF-IR and insulin receptor, respectively. The phosphorylation of IGF-IR and insulin receptor by their cognate ligands in the presence of BMS-554417, but not DMSO, was inhibited to nonstimulated levels. There was no change in the amount of IGF-IR or insulin receptor immunoprecipitated between the various treatment groups as determined by Western blotting for total receptors. In OV202 cells (Fig. 3*B*), there was no detectable phosphorylation of the immunoprecipitated insulin receptor in the presence or absence of growth factors (up to 50 nmol/L), which is consistent with previous data (20). There was detectable phosphorylation of the IGF-IR in cells that were incubated in serum-free medium. The degree of IGF-IR phosphorylation increased in response to treatment with LR3 IGF-I.

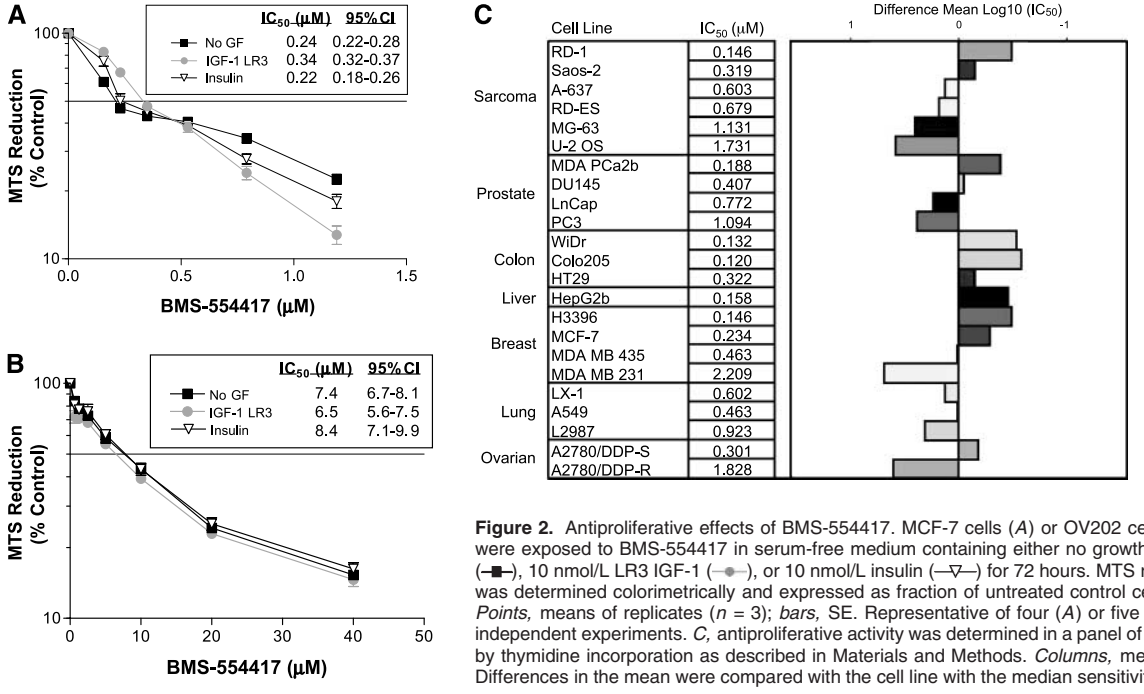

Figure 2. Antiproliferative effects of BMS-554417. MCF-7 cells (*A*) or OV202 cells (*B*) were exposed to BMS-554417 in serum-free medium containing either no growth factor (—■—), 10 nmol/L LR3 IGF-1 (—●—), or 10 nmol/L insulin (—▽—) for 72 hours. MTS reduction was determined colorimetrically and expressed as fraction of untreated control cells. *Points,* means of replicates ($n = 3$); *bars,* SE. Representative of four (*A*) or five (*B*) independent experiments. *C,* antiproliferative activity was determined in a panel of cell lines by thymidine incorporation as described in Materials and Methods. *Columns,* mean IC_{50}. Differences in the mean were compared with the cell line with the median sensitivity, A549.

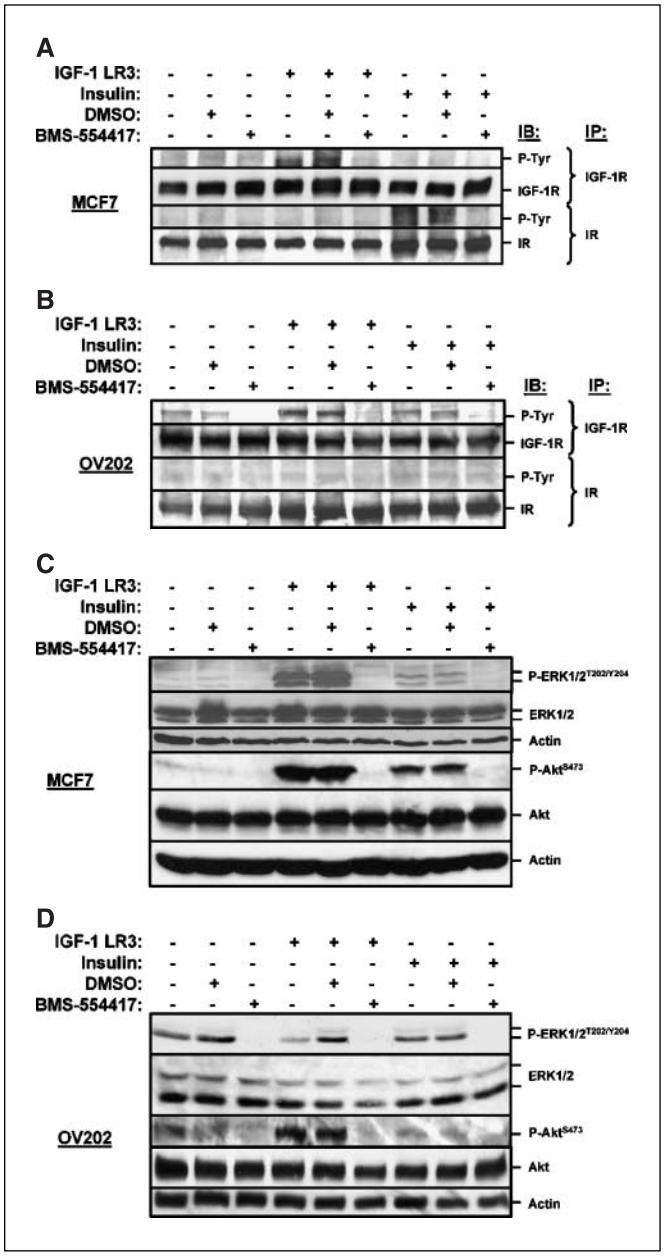

Figure 3. Inhibition of IGF-1R and insulin receptor phosphorylation and ERK/Akt pathways by BMS-554417. MCF-7 (*A* and *C*) or OV202 (*B* and *D*) cells in serum-free medium were treated with DMSO or BMS-554417 in the presence or absence of LR3 IGF-1 (10 nmol/L) or insulin (*A* and *B*: 25 nmol/L; *C* and *D*: 10 nmol/L). *A* and *B,* cells were lysed and the IGF-1R or insulin receptor (*IR*) was immunoprecipitated as described in Materials and Methods and probed using IGF-1Rβ or IRβ antibodies and phospho-specific antibodies against phosphotyrosine. *C* and *D,* cells were lysed and processed for Western blotting for total/phospho-specific ERK1/2 and total/phospho-specific Akt as described in Materials and Methods. Blots were probed for actin as a loading control.

Phosphorylation of IGF-IR in the presence or absence of growth factors was greatly reduced in the presence of BMS-554417 but not DMSO. As observed in MCF-7 cells, there was no appreciable change in the level of IGF-IR and insulin receptor among the various treatment groups.

BMS-554417 disrupts IGF-IR and insulin receptor signaling through the ERK and Akt pathways but not through p38 or JNK. To elucidate the mechanism by which BMS-554417 inhibits proliferation, we investigated the pathways known to be important in IGF-I and insulin-induced growth and mitogenesis (2, 34). Lysates were made from MCF-7 and OV202 cells treated with diluent or BMS-554417 in the absence or presence of LR3 IGF-I or insulin. In MCF-7 cells (Fig. 3*C*), there was relatively low phosphorylation of ERK1/2 and Akt in the unstimulated state. The addition of LR3 IGF-I and, to a lesser extent, insulin resulted in an increase in ERK1/2 phosphoinositide 3-kinase–dependent kinase-1 (PDK-1)–mediated phosphorylation of Akt at Ser^{473}. BMS-554417 inhibited this ligand-induced phosphorylation. In OV202 cells (Fig. 3*D*), ERK1/2 phosphorylation was detectable in the unstimulated state and was not as responsive to ligand stimulation. Nonetheless, BMS-554417 also inhibited ERK1/2 phosphorylation in both unstimulated and stimulated OV202 cells. PDK-1-mediated Akt phosphorylation was barely detectable in the unstimulated and insulin-treated OV202 cells. In the presence of LR3 IGF-I, Akt phosphorylation increased. BMS-554417 inhibited both stimulated and unstimulated Akt phosphorylation. Total ERK1/2 or Akt expression was not affected by any experimental conditions tested. Akt phosphorylation at Thr^{308}, which reflects phosphorylation by other kinases, was unaffected by treatment (data not shown). In both MCF-7 and OV202 cells, expression of p38 and JNK was not altered in response to LR3 IGF-I, insulin, DMSO, or BMS-554417. Phosphorylation of these kinases was undetectable after 2, 5, 10, 15, or 30 minutes of treatment (data not shown).

BMS-554417 abrogates IGF-I–mediated G_1 to S transition and nuclear accumulation of cyclin D1. IGF-I is a well-established mitogen that stimulates G_1 to S phase progression through phosphoinositide 3-kinase and ERK activation, increased cyclin D1 expression and nuclear localization, and retinoblastoma hyperphosphorylation (35). To investigate the ability of BMS-554417 to interfere with functional effects of IGF-I-mediated signaling, we analyzed MCF-7 cell cycle distribution and cyclin D1 localization in response to IGF-I with and without drug. MCF-7 cells in serum-free medium were either subjected to continuous growth in serum-free medium or LR3 IGF-I stimulation in the presence or absence of BMS-554417 for 24 hours (Fig. 4*A*). A small percentage of serum-deprived cells were found to be in the S phase (11.4 ± 2.0%). Stimulation with LR3 IGF-I induced a significant increase in S-phase cells (45.1 ± 8.8%). This S-phase increase was completely abolished by 5 μmol/L BMS-554417 (6.5 ± 2.6%). Similarly treated cells were stained for cyclin D1 expression and localization (Fig. 4*B*). Cells in serum-free medium expressed low levels of cyclin D1, which seemed largely excluded from the nucleus. Upon stimulation with LR3 IGF-I, there was a dramatic increase in overall cyclin D1 expression and intense nuclear staining. Upon concurrent treatment with BMS-554417, the effects of LR3 IGF-I on overall cyclin D1 staining intensity and nuclear localization were dramatically reduced.

MCF-7 and OV202 cells undergo apoptotic cell death upon BMS-554417 exposure. Because BMS-554417 treatment decreased MTS dye reduction and inhibited IGF-I-induced activation of Akt, a kinase that regulates apoptosis in a number of ways (14), we investigated whether BMS-554417 treatment could initiate apoptosis. MCF-7 and OV202 cells were incubated in serum-free medium in the absence or presence of BMS-554417. After treatment, both adherent and nonadherent cells were collected and subjected to Western blotting with antibodies to PARP-1, a caspase substrate that is cleaved in

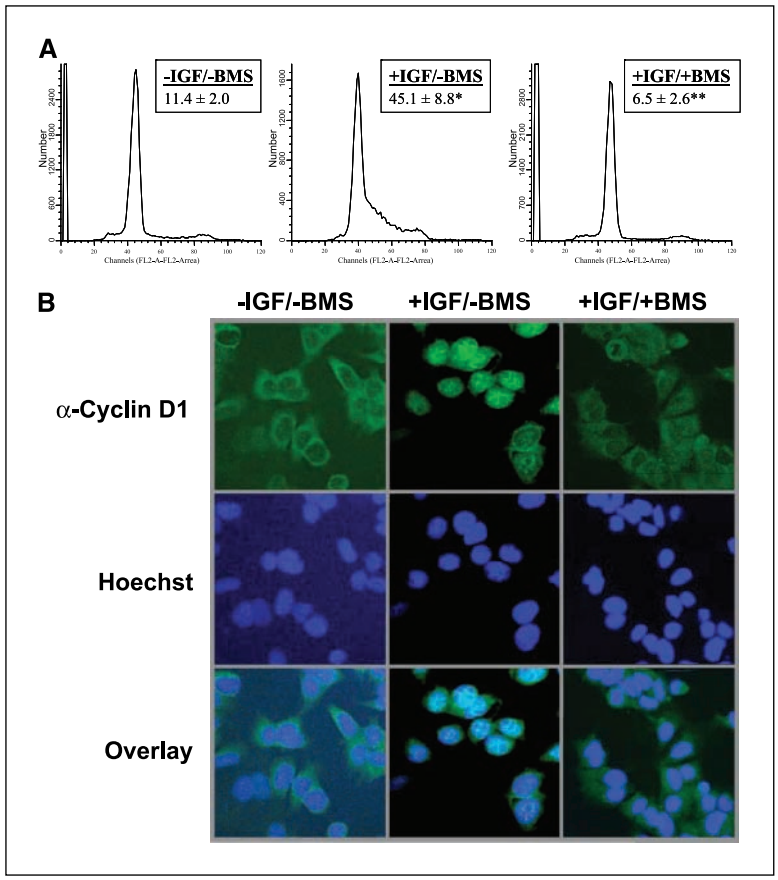

Figure 4. BMS-554417 inhibits IGF-1 stimulated cell cycle progression and cyclin D1 nuclear accumulation in MCF-7 cells. Subconfluent MCF-7 cells were exposed to either serum-free medium, 10 nmol/L LR3 IGF-1 or 10 nmol/L LR3 IGF-1 plus 5 μmol/L BMS-554417 for 24 hours. Cells were either harvested and analyzed for cell cycle distribution by fluorescence-activated cell sorting analysis (*A*) or stained for cyclin D1 (*B*) as described in Materials and Methods. Representative fields taken at ×63. *Points,* S-phase mean of three independent experiments; *bars,* SD. *, $P < 0.05$ versus −IGF/−BMS; **, $P < 0.05$ versus +IGF/−BMS.

a variety of cells undergoing apoptosis (Fig. 5*A*) or examined for apoptotic morphologic changes (Fig. 5*B*; refs. 36–38). Both MCF-7 and OV202 cells exhibited PARP-1 cleavage and nuclear fragmentation in response to BMS-554417 treatment but not DMSO.

BMS-554417–induced caspase activation occurs through the mitochondrial pathway. We then decided to elucidate the biochemical pathway involved in BMS-554417-induced apoptosis. As indicated previously, IGF-IR- and insulin receptor–initiated signals can inhibit both the mitochondrial and death receptor pathways. Conversely, inhibition of IGFR1 and insulin receptor signaling might facilitate activation of either pathway. In view of recent data showing activity of IGR-1R inhibitors against leukemia (39) and the availability of a variety of isogenic Jurkat leukemia cell lines differing in expression of only one or two pathway components, studies examining BMS-554417-induced death pathway activation were done in this cell type.

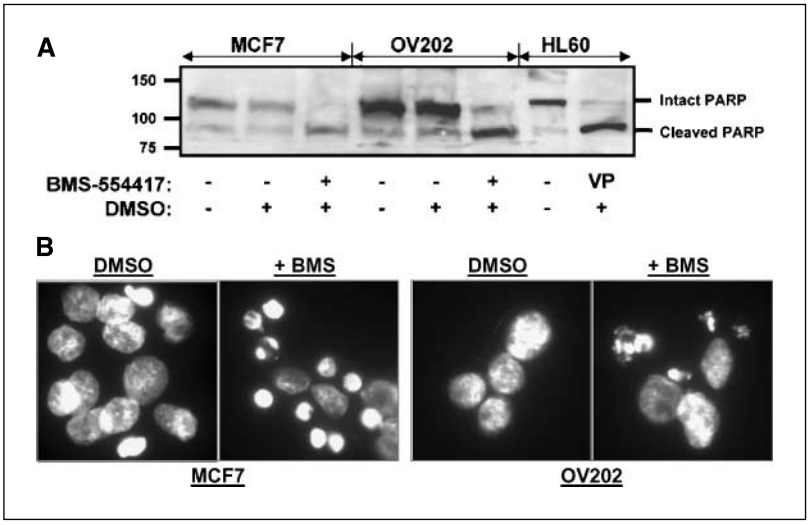

Figure 5. BMS-554417-treated MCF-7 and OV202 cells exhibit hallmarks of apoptosis. MCF-7 and OV202 cells treated with BMS-554417 or DMSO were either (*A*) lysed and analyzed by Western blotting using an antibody that detects full length PARP-1, as well as the cleaved fragments or (*B*) harvested and visualized by fluorescence microscopy in the presence of 1 μg/mL Hoechst 33258 (*A*). HL-60 lysates treated for 6 hours in the absence or presence of 68 nmol/L etoposide were run as negative and positive controls. Representative blot of triplicate experiments. Representative images of cell populations taken at ×63.

As shown in Fig. 6*A*, Jurkat cells and their variants expressed both IGF-IR and insulin receptor. MTS assays showed that BMS-554417 exhibited dose-dependent antiproliferative effects in parental Jurkat cells with and IC_{50} of 9 ± 1 μmol/L (n = 7; Fig. 6*B*). After 72 hours of drug treatment, the percentage of cells with apoptotic morphologic changes (illustrated in Fig. 6*C, inset*) also increased in a dose-dependent manner (Fig. 6*C*). To assess the possibility that induction of apoptosis reflected BMS-554417-induced activation of the death receptor pathway, Jurkat cells were treated with BMS-554417 in the presence of Nok1, a neutralizing antibody to Fas ligand (40); a death receptor 5:Fc fusion protein, which blocks TRAIL-induced receptor activation (41, 42); or the caspase-8-selective inhibitor IETD(OMe)-fmk, which inhibits the death receptor pathway preferentially at low concentrations (41). None of these treatments inhibited BMS-554417-induced apoptosis in Jurkat cells. However, treatment with the broad-spectrum caspase inhibitor ZV4D (OMe)-fmk inhibited the induction of apoptosis in Jurkat cells treated with BMS-554417 (Fig. 6*D*; ref. 43). Consistent with these results, a Jurkat variant lacking expression of FADD (I2.1 cells), the adaptor required for death receptor–initiated caspase activation (44), remained sensitive to BMS-554417 (Fig. 6*E*). In contrast, forced overexpression of Bcl-2 (JB-6 cells) or Bcl-x_L (5B4 cells) markedly diminished sensitivity to BMS-554417-induced apoptosis in Jurkat cells (Fig. 6*E*; refs. 45, 46). Collectively, these results suggest that BMS-554417 induces apoptosis in Jurkat cells by a process that does not involve Fas ligand, TRAIL, or FADD but does involve the mitochondrial pathway of caspase activation.

BMS-554417 shows activity *in vivo*. To investigate the activity of BMS-554417 *in vivo*, we used a mouse allograft model (IGF-IR Sal) that expressed a consitutively activated IGF-IR (31). Fourteen days after s.c. implantation of IGF-IR Sal tumor fragments, mice were treated with vehicle in the absence or presence of BMS-554417 at 200 mg/kg/dose. This resulted in significant antitumor activity as measured by decrease in days to target volume (19.3 versus 35.5, P = 0.0004) and mean tumor volume at days 17 to 28 (Fig. 7*A*). The concentration of BMS-554417 (mean ± SD) detected in the serum of treated mice at 6 hours after administration was 30.0 ± 4.16 μmol/L. This concentration was significantly higher than the IC_{50} of the most resistant cell line tested (OV202, P = 0.0007).

To evaluate the acute metabolic effects of BMS-554417 *in vivo*, we did an oral glucose tolerance test (OGTT) on mice treated with vehicle alone or with BMS-554417 at 200 mg/kg (Fig. 7*B*). Before administration of the glucose load, there was a small but

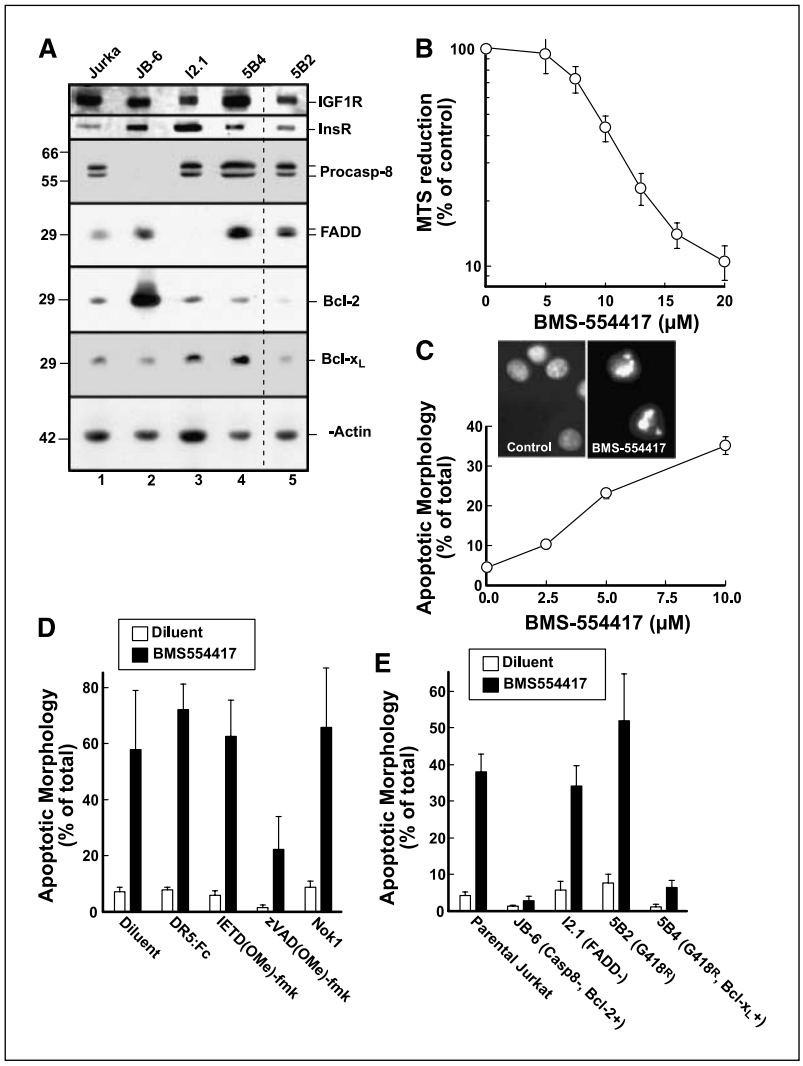

Figure 6. Effect of BMS-554417 on Jurkat cell variants. *A,* aliquots containing 50 μg of total cellular protein from the indicated cell lines were subjected to SDS-PAGE followed by immunoblotting with reagents that recognized the indicated polypeptide species. *B,* Jurkat cells were incubated for 72 hours in the presence of increasing concentrations of BMS-554417, then assayed for their ability to reduce MTS. *Points,* % diluent-treated control samples subjected to the same incubation. *C,* Jurkat cells were treated with the indicated BMS-554417 concentration for 72 hours and examined for apoptotic morphological changes. *Inset,* parental Jurkat cells were treated with 0.1% DMSO (*Control*) or 10 μmol/L BMS-554417 and examined for apoptotic morphology. *D,* parental Jurkat cells were treated with diluent or 10 μmol/L BMS-554417 for 72 hours in the absence or presence of 1,000 ng/mL DR5:Fc, a synthetic decoy receptor for TRAIL; 10 μmol/L IETD(OMe)-fmk, a synthetic caspase inhibitor that preferentially inhibits caspases-8 and caspase-10; 50 μmol/L zVAD(OMe)-fmk, a broad spectrum caspase inhibitor; or 1 mg/mL Nok-1, a FasL-blocking antibody. *E,* parental Jurkat cells or Jurkat variants lacking caspase-8 and overexpressing Bcl-2 (JB-6), lacking FADD (I2.1), overexpressing Bcl-x_L (clone 5B4), or empty vector (clone 5B2) were incubated for 72 hours with 0.1% DMSO (*open columns*) or 10 μmol/L BMS-554417 (*closed columns*). Similar results were obtained with an additional Bcl-x_L overexpressing clone. *Bars,* SD from three to seven independent experiments (*B, C, D*, and *E*).

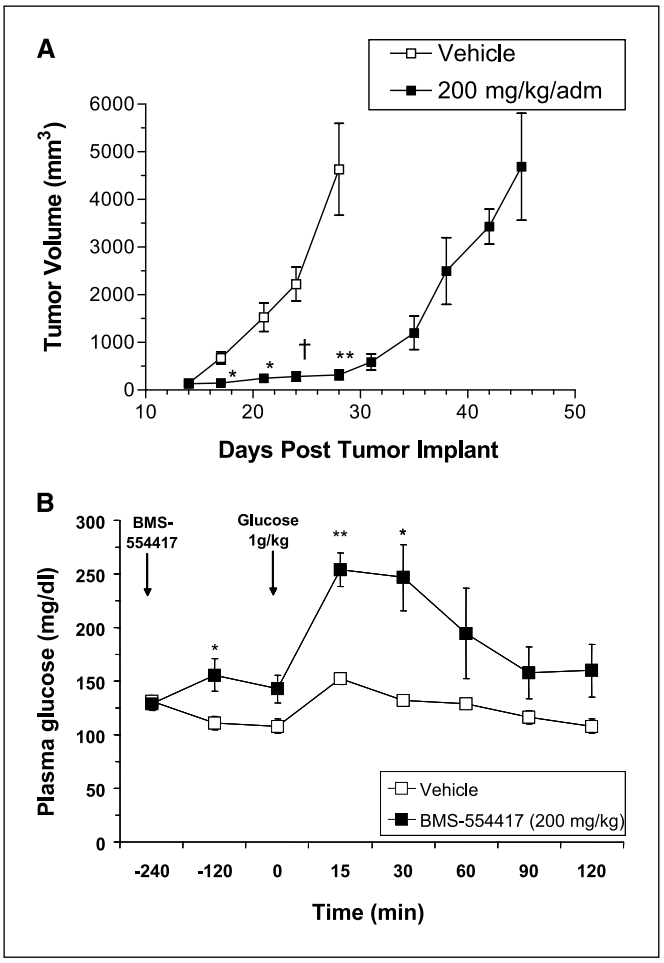

Figure 7. BMS-554417 shows oral antitumor activity *in vivo* in IGF-IR Sal tumor allografts with transient hyperglycemia. *A,* tumors were established in nude mice by s.c. injection of IGF-IR Sal tumor fragments from donor mice. Fourteen days after implantation (tumor volume, ~100 mm^3), mice received twice daily oral dosing of vehicle (polyethylene glycol 400/distilled water, 80:20) or BMS-554417 at 200 mg/kg for 14 days. *Points,* mean tumor volumes of eight animals; *bars,* SE. *, $P < 0.005$; **, $P < 0.001$; †, $P < 0.0005$. *B,* after a 2-hour fasting period, mice were dosed orally with vehicle alone (polyethylene glycol 400/distilled water, 80:20) or BMS-554417 at 200 mg/kg in a single dose 4 hours before glucose challenge (1 g/kg). Serum was collected as described in Materials and Methods and analyzed for glucose, insulin, and BMS-554417. *Points,* mean of five mice; *bars,* SE. *, $P < 0.05$; **, $P < 0.005$.

statistically significant increase in serum glucose in response to BMS-554417. Upon administration of the glucose load, there was an increase in serum glucose that remained significantly higher in the BMS-554417-treated animals than vehicle controls for 30 minutes. At 2 hours after glucose load, the serum insulin level (mean ± SD) was significantly elevated in BMS-554417-treated animals (67.7 ± 10.3 ng/mL) compared with control (0.152 ± 0.0779 ng/mL, $P = 0.0001$).

Discussion

BMS-554417 is the first dual-kinase small-molecule inhibitor of the IGF-IR and insulin receptor to show antiproliferative and proapoptotic activity in multiple cell types. The inhibition of IGF-IR and insulin receptor phosphorylation in treated cells was consistent with the similar degree of potent inhibition of the IGF-IR and insulin receptor in cell-free kinase assays. It seemed that inhibition of both kinases occurred without down-regulation of IGF-IR or insulin receptor protein expression. BMS-554417 had antiproliferative effects in multiple cancer cell line types and did not seem to require the addition of stimulatory ligands for this effect in MCF-7 or OV202 cells.

Using *in vitro* kinase assays, BMS-554417 also seemed to be a potent inhibitor of the FAK kinase activity. To test the ability of BMS-554417 to inhibit FAK in intact cells, we measured FAK phosphorylation at Tyr^{397}, which is the major FAK autophosphorylation site and is important for FAK catalytic activity, binding of SH2 and Src family kinases, activation of focal adhesion proteins, and binding of the FAK-binding proteins Cas and Paxillin (47). Surprisingly, at doses that inhibited proliferation in MCF-7 and OV202 cells, BMS-554417 did not seem to affect the phosphorylation of FAK at Tyr^{397} in treated cells (data not shown). FAK expression and phosphorylation at Tyr^{397} was also not detectably altered by the presence of LR3 IGF-I or insulin (data not shown). Thus, under the conditions investigated in MCF-7 and OV202 cells, FAK may not be playing a major role in IGF-I signaling. It is conceivable that in other models where FAK plays a significant role in IGF-I or insulin-mediated signaling, an inhibitory effect may be observed (48). Alternatively, the recombinant FAK fragment used in the *in vitro* kinase assays may have a conformation and selectivity that differs from the native enzyme, as has been observed in similar studies with kinase inhibitors (49).

Consistent with the known role of the IGF-I system in cancer cells, treatment with BMS-554417 resulted in inhibition of ERK1/2 and Akt phosphorylation, diminution of IGF-I-mediated proliferation, and stimulation of apoptosis. Because ligation of IGF-IR and insulin receptor leads to activation of the serine/threonine kinase Akt, which can inhibit both the death receptor and mitochondrial pathways (14), it was not clear how treatment with BMS-554417 might lead to apoptosis. On one hand, inhibition of IGF-IR and insulin receptor signaling could potentially lead to increased expression of Fas ligand (50), which could induce caspase activation through the Fas receptor in an autocrine or paracrine fashion (51–54). Treatment of Jurkat cells with a variety of agents that inhibit the death receptor pathway, including the blocking antibody Nok-1 and the caspase-8-selective inhibitor IETD(OMe)-fmk, failed to inhibit BMS-554417-induced apoptosis (Fig. 6*D*). Likewise, loss of FADD expression failed to affect BMS-554417-induced apoptosis (Fig. 6*D*). Collectively, these results argue that BMS-554417-induced activation of death ligand expression is unlikely to be a major cause of the cytotoxicity induced by this agent. In contrast, overexpression of Bcl-2 or Bcl-x_L markedly diminished the cytotoxicity of BMS-554417 (Fig. 6*E*). These results not only suggest that BMS-554417 is inducing apoptosis in Jurkat cells by activating the mitochondrial pathway but also identify a potential mechanism of resistance to this agent.

At the most effective dose of BMS-554417 tested (200 mg/kg), transient hyperglycemia and supraphysiologic elevations of secreted insulin was observed. At lower doses of 80 and 120 mg/kg, we did observe modest increases in insulin (2.82 ± 0.950 and 5.97 ± 1.64 ng/mL, respectively), but this was not associated with hyperglycemia was not observed (data not shown). These results suggest that mice hypersecrete insulin in response to BMS-554417 as a compensatory mechanism. At increasing drug doses, it seems a critical threshold is reached, overwhelming this adaptive mechanism and hyperglycemia ensues. This phenomenon could

be used as a marker of a target effect of BMS-554417. Because this was a single-dose study, it is unclear if chronic exposure to BMS-554417 would cause more prolonged hyperglycemia or other adverse metabolic consequences. On the other hand, no weight loss was observed in the cohort of mice treated at the 200 mg/kg dose level. Further studies will be needed to define this potentially compensatory mechanism. In summary, BMS-554417 represents a member of a novel class of potent dual-kinase inhibitors of the IGF-IR and insulin receptor. Due to the dependence of multiple hematologic and nonhematologic malignancies on the IGF-I system for proliferation and inhibition of apoptosis, members of this drug class represent a potentially promising therapy. Furthermore, due to the effect of the IGF-I system on resistance to standard agents used in the treatment of cancer, studies combining dual-kinase inhibitors of the IGF-I system, such as BMS-554417 with chemotherapy, biological and hormonal agents, or radiation, might represent interesting combinations for future preclinical investigations.

Acknowledgments

Received 3/31/2005; revised 8/30/2005; accepted 10/5/2005.

Grant support: R01 CA69008 (S.H. Kaufmann) and Clinician Investigator Program of the Mayo Clinic (P. Haluska).

The costs of publication of this article were defrayed in part by the payment of page charges. This article must therefore be hereby marked *advertisement* in accordance with 18 U.S.C. Section 1734 solely to indicate this fact.

We thank the Mayo Clinic Flow Cytometry/Optical Morphology Share Resource for their help with cell cycle analysis and confocal microscopy, Sumithra Mandrekar and Alfred Furth for statistical support, Aixin Li for selectivity testing and insulin measurements, Lorell Discenza for serum determinations of BMS-554417, Ann Greer for antiproliferative thymidine assays, Janet Dell for performing the OGTT assay, and Laura E. Wuotila for secretarial support.

References

1. Baserga R, Peruzzi F, Reiss K. The IGF-1 receptor in cancer biology. Int J Cancer 2003;107:873–7.
2. Dupont J, LeRoith D. Insulin and insulin-like growth factor I receptors: similarities and differences in signal transduction. Horm Res 2001;55Suppl 2:22–6.
3. LeRoith D, Roberts CT, Jr. The insulin-like growth factor system and cancer. Cancer Lett 2003;195: 127–37.
4. Pandini G, Frasca F, Mineo R, Sciacca L, Vigneri R, Belfiore A. Insulin/insulin-like growth factor I hybrid receptors have different biological characteristics depending on the insulin receptor isoform involved. J Biol Chem 2002;277:39684–95.
5. Pollak MN, Schernhammer ES, Hankinson SE. Insulin-like growth factors and neoplasia. Nat Rev Cancer 2004; 4:505–18.
6. Kalli KR, Conover CA. The insulin-like growth factor/ insulin system in epithelial ovarian cancer. Front Biosci 2003;8:d714–22.
7. Bohula EA, Playford MP, Macaulay VM. Targeting the type 1 insulin-like growth factor receptor as anti-cancer treatment. Anticancer Drugs 2003;14:669–82.
8. Lu Y, Zi X, Pollak M. Molecular mechanisms underlying IGF-I-induced attenuation of the growth-inhibitory activity of trastuzumab (Herceptin) on SKBR3 breast cancer cells. Int J Cancer 2004;108:334–41.
9. Beech DJ, Perer E, Helms J, Gratzer A, Deng N. Insulin-like growth factor-I receptor activation blocks doxorubicin cytotoxicity in sarcoma cells. Oncol Rep 2003;10: 181–4.
10. Camirand A, Lu Y, Pollak M. Co-targeting HER2/ ErbB2 and insulin-like growth factor-1 receptors causes synergistic inhibition of growth in HER2-overexpressing breast cancer cells. Med Sci Monit 2002;8:BR521–6.
11. Sun HZ, Wu SF, Tu ZH. Blockage of IGF-1R signaling sensitizes urinary bladder cancer cells to mitomycin-mediated cytotoxicity. Cell Res 2001;11:107–15.
12. Yee D, Kern FG, Spang-Thomsen M, Lippman ME, Cullen KJ, Wiseman LR. Type I IGF receptor and acquired tamoxifen resistance in oestrogen-responsive human breast cancer cells. Eur J Cancer 1993;29A: 562–9.
13. Peretz S, Jensen R, Baserga R, Glazer PM. ATM-dependent expression of the insulin-like growth factor-I receptor in a pathway regulating radiation response. Proc Natl Acad Sci U S A 2001;98:1676–81.
14. Datta SR, Brunet A, Greenberg ME. Cellular survival: a play in three Akts. Genes Dev 1999;13:2905–27.
15. Datta SR, Dudek H, Tao X, et al. Akt phosphorylation of BAD couples survival signals to the cell-intrinsic death machinery. Cell 1997;91:231–41.
16. Dijkers PF, Medema RH, Lammers JW, Koenderman L, Coffer PJ. Expression of the pro-apoptotic Bcl-2 family member Bim is regulated by the forkhead transcription factor FKHR-L1. Curr Biol 2000;10:1201–4.
17. Kennedy SG, Kandel ES, Cross TK, Hay N. Akt/ Protein kinase B inhibits cell death by preventing the release of cytochrome *c* from mitochondria. Mol Cell Biol 1999;19:5800–10.
18. Cardone MH, Roy N, Stennicke HR, et al. Regulation of cell death protease caspase-9 by phosphorylation. Science 1998;282:1318–21.
19. Zhang H, Yee D. The therapeutic potential of agents targeting the type I insulin-like growth factor receptor. Expert Opin Investig Drugs 2004;13:1569–77.
20. Kalli KR, Falowo OI, Bale LK, Zschunke MA, Roche PC, Conover CA. Functional insulin receptors on human epithelial ovarian carcinoma cells: implications for IGF-II mitogenic signaling. Endocrinology 2002;143: 3259–67.
21. Vella V, Pandini G, Sciacca L, et al. A novel autocrine loop involving IGF-II and the insulin receptor isoform-A stimulates growth of thyroid cancer. J Clin Endocrinol Metab 2002;87:245–54.
22. Sciacca L, Mineo R, Pandini G, Murabito A, Vigneri R, Belfiore A. In IGF-I receptor-deficient leiomyosarcoma cells autocrine IGF-II induces cell invasion and protection from apoptosis via the insulin receptor isoform A. Oncogene 2002;21:8240–50.
23. Finlayson CA, Chappell J, Leitner JW, et al. Enhanced insulin signaling via Shc in human breast cancer. Metabolism 2003;52:1606–11.
24. Milazzo G, Giorgino F, Damante G, et al. Insulin receptor expression and function in human breast cancer cell lines. Cancer Res 1992;52:3924–30.
25. Wolford ST, Schroer RA, Gohs FX, et al. Reference range data base for serum chemistry and hematology values in laboratory animals. J Toxicol Environ Health 1986;18:161–88.
26. Juo P, Kuo CJ, Yuan J, Blenis J. Essential requirement for caspase-8/FLICE in the initiation of the Fas-induced apoptotic cascade. Curr Biol 1998;8:1001–8.
27. Kawahara A, Ohsawa Y, Matsumura H, Uchiyama Y, Nagata S. Caspase-independent cell killing by Fas-associated protein with death domain. J Cell Biol 1998; 143:1353–60.
28. Parrizas M, Gazit A, Levitzki A, Wertheimer E, LeRoith D. Specific inhibition of insulin-like growth factor-1 and insulin receptor tyrosine kinase activity and biological function by tyrphostins. Endocrinology 1997; 138:1427–33.
29. Smith P, Krohn R, Hermanson G, et al. Measurement of protein using bicinchoninic acid. Anal Biochem 1985; 150:76–85.
30. Kottke TJ, Blajeski AL, Martins LM, et al. Comparison of paclitaxel-, 5-fluoro-2′-deoxyuridine-, and epidermal growth factor (EGF)-induced apoptosis. Evidence for EGF-induced anoikis. J Biol Chem 1999;274:15927–36.
31. Carboni JM, Lee AV, Hadsell DL, et al. Tumor development by transgenic expression of a constitutively active insulin-like growth factor-1 receptor. Cancer Res 2005;65:3781–7.
32. Wittman M, Carboni J, Attar R, et al. Discovery of a (1H-benzoimidazol-2-yl)-1H-pyridin-2-one (BMS-536924) inhibitor of insulin-like growth factor I receptor kinase with *in vivo* antitumor activity. J Med Chem 2005;48:5639–43.
33. Francis GL, Ross M, Ballard FJ, et al. Novel recombinant fusion protein analogues of insulin-like growth factor (IGF)-I indicate the relative importance of IGF-binding protein and receptor binding for enhanced biological potency. J Mol Endocrinol 1992;8: 213–23.
34. Le Roith D, Bondy C, Yakar S, Liu JL, Butler A. The somatomedin hypothesis: 2001. Endocr Rev 2001;22: 53–74.
35. Hamelers IH, van Schaik RF, Sipkema J, Sussenbach JS, Steenbergh PH. Insulin-like growth factor I triggers nuclear accumulation of cyclin D1 in MCF-7S breast cancer cells. J Biol Chem 2002;277:47645–52.
36. Lazebnik YA, Kaufmann SH, Desnoyers S, Poirier GG, Earnshaw WC. Cleavage of poly(ADP-ribose) polymerase by a proteinase with properties like ICE. Nature 1994; 371:346–7.
37. Kaufmann SH, Desnoyers S, Ottaviano Y, Davidson NE, Poirier GG. Specific proteolytic cleavage of poly(ADP-ribose) polymerase: an early marker of chemotherapy-induced apoptosis. Cancer Res 1993;53: 3976–85.
38. Kottke TJ, Blajeski AL, Meng XW, et al. Lack of correlation between caspase activation and caspase activity assays in paclitaxel-treated MCF-7 breast cancer cells. J Biol Chem 2002;277:804–15.
39. Mitsiades CS, Mitsiades NS, McMullan CJ, et al. Inhibition of the insulin-like growth factor receptor-1 tyrosine kinase activity as a therapeutic strategy for multiple myeloma, other hematologic malignancies, and solid tumors. Cancer Cell 2004;5:221–30.
40. Kayagaki N, Kawasaki A, Ebata T, et al. Metalloproteinase-mediated release of human Fas ligand. J Exp Med 1995;182:1777–83.
41. Meng XW, Chandra J, Loegering D, et al. Central role of Fas-associated death domain protein in apoptosis induction by the mitogen-activated protein kinase kinase inhibitor CI-1040 (PD184352) in acute lymphocytic leukemia cells *in vitro*. J Biol Chem 2003;278: 47326–39.
42. Kalli KR, Devine KE, Cabot MC, et al. Heterogeneous role of caspase-8 in fenretinide-induced apoptosis in epithelial ovarian carcinoma cell lines. Mol Pharmacol 2003;64:1434–43.
43. Slee EA, Zhu H, Chow SC, MacFarlane M, Nicholson DW, Cohen GM. Benzyloxycarbonyl-Val-Ala-Asp (OMe) fluoromethylketone (Z-VAD.FMK) inhibits apoptosis by blocking the processing of CPP32. Biochem J 1996;315: 21–4.
44. Sprick MR, Rieser E, Stahl H, Grosse- Wilde A, Weigand MA, Walczak H. Caspase-10 is recruited to and activated at the native TRAIL and CD95 death-inducing

signalling complexes in a FADD-dependent manner but can not functionally substitute caspase-8. EMBO J 2002; 21:4520–30.
45. Yang J, Liu X, Bhalla K, et al. Prevention of apoptosis by Bcl-2: release of cytochrome *c* from mitochondria blocked.[see comment]. Science 1997;275:1129–32.
46. Ibrado AM, Liu L, Bhalla K. Bcl-xL overexpression inhibits progression of molecular events leading to paclitaxel-induced apoptosis of human acute myeloid leukemia HL-60 cells. Cancer Res 1997;57:1109–15.
47. Parsons JT. Focal adhesion kinase: the first ten years. J Cell Sci 2003;116:1409–16.
48. Baron V, Calleja V, Ferrari P, Alengrin F, Van Obberghen E. p125Fak focal adhesion kinase is a substrate for the insulin and insulin-like growth factor-I tyrosine kinase receptors. J Biol Chem 1998; 273:7162–8.
49. Garcia-Echeverria C, Pearson MA, Marti A, et al. *In vivo* antitumor activity of NVP-AEW541-A novel, potent, and selective inhibitor of the IGF-IR kinase. Cancer Cell 2004;5:231–9.
50. Brunet A, Bonni A, Zigmond MJ, et al. Akt promotes cell survival by phosphorylating and inhibiting a Forkhead transcription factor. Cell 1999;96:857–68.
51. Friesen C, Herr I, Krammer PH, Debatin KM. Involvement of the CD95 (APO-1/FAS) receptor/ligand system in drug-induced apoptosis in leukemia cells. Nat Med 1996;2:574–7.
52. Fulda S, Los M, Friesen C, Debatin KM. Chemosensitivity of solid tumor cells *in vitro* is related to activation of the CD95 system. Int J Cancer 1998;76:105–14.
53. Fulda S, Meyer E, Friesen C, Susin SA, Kroemer G, Debatin KM. Cell type specific involvement of death receptor and mitochondrial pathways in drug-induced apoptosis. Oncogene 2001;20:1063–75.
54. Fulda S, Sieverts H, Friesen C, Herr I, Debatin KM. The CD95 (APO-1/Fas) system mediates drug-induced apoptosis in neuroblastoma cells. Cancer Res 1997;57: 3823–9.